

TU-608  
 YITP-00-73  
 hep-ph/0012279  
 December 2000

# Radiative decay of a massive particle and the non-thermal process in primordial nucleosynthesis

Masahiro Kawasaki

*Research Center for the Early Universe, School of Science, University of Tokyo, Tokyo 113-0033, Japan*

Kazunori Kohri

*Yukawa Institute for Theoretical Physics, Kyoto University, Kyoto, 606-8502, Japan*

Takeo Moroi

*Department of Physics, Tohoku University, Sendai 980-8578, Japan*

## Abstract

We consider the effects on big bang nucleosynthesis (BBN) of the radiative decay of a long-lived massive particle. If high-energy photons are emitted after the BBN epoch ( $t \sim 1 - 10^3$  sec), they may change the abundances of the light elements through photodissociation processes, which may result in a significant discrepancy between standard BBN and observation. Taking into account recent observational and theoretical developments in this field, we revise our previous study constraining the abundance of the radiatively-decaying particles. In particular, on the theoretical side, it was recently claimed that the non-thermal production of  ${}^6\text{Li}$ , which is caused by the photodissociation of  ${}^4\text{He}$ , most severely constrains the abundance of the radiatively-decaying particle. We will see, however, it is premature to emphasize the importance of the non-thermal production of  ${}^6\text{Li}$  because (i) the theoretical computation of the  ${}^6\text{Li}$  abundance has large uncertainty due to the lack of the precise understanding of the  ${}^6\text{Li}$  production cross section, and (ii) the observational data of  ${}^6\text{Li}$  abundance has large errors.

Typeset using REVTeX

## I. INTRODUCTION

Big-bang nucleosynthesis (BBN) is one of the most important tools to probe the early universe. Because it is very sensitive to the condition of the universe from  $10^{-2}$  sec to  $10^{12}$  sec, we can indirectly check the history of the universe and impose constraints on a hypothetical particles by the observational light element abundances.

There are a lot of models of the modern particle physics beyond the standard model, e.g. supergravity or superstring theory, which predict unstable massive particles with masses of  $\mathcal{O}(100 \text{ GeV})$ , such as gravitino, Polonyi field, moduli, and so on. They have long lifetimes because their interactions are suppressed by inverse powers of the gravitational scale. Consequently, these exotic particles may decay at about the BBN epoch ( $T \lesssim 1\text{MeV}$ ). If the massive particles radiatively decays, the emitted high energy photons induce the electromagnetic cascade process. If the decay occurs after the BBN starts, the light elements would be destroyed by the cascade photons and their abundances would be changed significantly. Comparing the theoretically predicted light element abundances with the observational ones, we can impose constraints on the energy density, the mass, and the lifetime of the parent massive particle [1–3]. In particular, Holtmann and the present authors [3] performed the Maximum Likelihood analysis including both theoretical and observational errors and obtained the precise constraints.

After Ref. [3] was published, several new observational data of light elements were reported. As for the  $^4\text{He}$  abundance, it was still unclear whether the observational value of the primordial  $^4\text{He}$  mass fraction  $Y$  is low ( $\sim 0.234$ ) [4,5] or high ( $\sim 0.244$ ) [6]. However, Fields and Olive considered the HeI absorption effect and reanalyzed the data [7], and they obtained a relatively middle value of  $Y$  ( $\sim 0.238$ ). On the other hand, as for the primordial D/H, although low values of D/H ( $\sim 10^{-5}$ ) [8] had been measured and regarded as the primordial abundance, a relatively high value of D/H ( $\sim 10^{-4}$ ) was claimed again by Tytler et al. in the high redshift QSO absorption systems [9]. In their paper they stressed that while the data may be inadequate to definitely conclude it to be precise value, there is still a possibility of the high D/H.

On the theoretical side, recently it was claimed that the severest constraint on the radiatively-decaying particle may be from the non-thermal production of  $^6\text{Li}$ , which is a secondary  $^6\text{Li}$  production due to the background  $^4\text{He}$  and the energetic T or  $^3\text{He}$  produced by the  $^4\text{He}$  photodissociation.<sup>1</sup> However, the observational data of the primordial component of  $^6\text{Li}$  has large uncertainties. In addition, precise experimental data for the nuclear cross sections are not available. Therefore, it is unclear how important the non-thermal  $^6\text{Li}$  production is once we take account of these uncertainties.

With these new developments in theory and observation, we revise the previous constraint on the radiative decay of long-lived particles. We obtain the photon spectrum by solving the Boltzmann equation numerically [2]. In addition we perform the Monte Carlo simulation which includes both the experimental and theoretical errors. Then, we estimate the confidence levels by performing the Maximum Likelihood method including both the

---

<sup>1</sup>Such a possibility of the secondary process had already been pointed out by the earlier works for hadronic decaying particles [11].

theoretical and the observational errors.

This paper is organized as follows. In Sec. II we briefly review the current status of the observational data. In Sec. III we introduce the formulations for the photodissociation and non-thermal  ${}^6\text{Li}$  production. In Sec. IV we compare the theoretical predictions with the observations. Sec V is devoted to conclusions.

## II. OBSERVATIONAL LIGHT ELEMENT ABUNDANCES

Here we summarize the current status of the observational light element abundances. The primordial D/H is measured in the high redshift QSO absorption systems. Recently a new deuterium data was obtained from observation of QSO HS 0105+1619 at  $z = 2.536$  [12]. It was found that the cloud is neutral and has a simple structure. Five Lyman series transitions caused by D and H were observed there. The reported value of the deuterium abundance was relatively low,  $(\text{D}/\text{H})^{\text{obs}} = (2.54 \pm 0.23) \times 10^{-5}$ . Combined with the previous “Low D” data which were obtained by the clouds at  $z = 3.572$  towards Q1937-1009 and at  $z = 2.504$  towards Q1009+2956 [8], the primordial abundance is obtained as

$$\text{LowD} : (\text{D}/\text{H})^{\text{obs}} = (3.0 \pm 0.4) \times 10^{-5}. \quad (1)$$

We call this value “Low D.” On the other hand, Webb et al. observed high deuterium abundance in relatively low redshift absorption systems at  $z = 0.701$  towards Q1718+4807 [13],

$$\text{HighD} : (\text{D}/\text{H})^{\text{obs}} = (2.0 \pm 0.5) \times 10^{-4}. \quad (2)$$

Tytler et al. [9] also observed the clouds independently and obtained the similar value. Since Webb et al. and Tytler et al. did not obtain the full spectra of the Lyman series in their observations, the precise fitting of D/H based on the “High D” data might be inadequate. However, the possibility of “High D” have not been excluded yet. Therefore, we also consider the possibility of “High D” and include it in our analysis.

For  ${}^3\text{He}$ , we use the pre-solar measurements. In this paper, we do not rely upon models of galactic and stellar chemical evolution because of the large uncertainty in extrapolating back to the primordial abundance. But it is reasonable to assume that  ${}^3\text{He}/\text{D}$  is an increasing function of the cosmic time, because D is the most fragile isotope and is always destroyed whenever  ${}^3\text{He}$  is destroyed. Using the solar-system data reanalyzed by Geiss [14],

$$r_{3,2,\odot}^{\text{obs}} \equiv \left( {}^3\text{He}/\text{D} \right)_{\odot}^{\text{obs}} = 0.591 \pm 0.536, \quad (3)$$

where  $\odot$  denotes the pre-solar abundance. We take this to be an upper bound on the primordial  ${}^3\text{He}$  to D ratio  $r_{3,2}^{\text{obs}}$ :

$$r_{3,2}^{\text{obs}} \leq r_{3,2,\odot}^{\text{obs}}. \quad (4)$$

Although in the standard scenario the theoretical prediction satisfies the above constraint,  ${}^4\text{He}$  photodissociation produces both D and  ${}^3\text{He}$  and can raise the  ${}^3\text{He}$  to D ratio [15]. Hence, we include this constraint into our analysis.

The primordial  ${}^4\text{He}$  mass fraction  $Y$  is inferred from observation of recombination lines from the low metallicity extragalactic HII regions. Since  ${}^4\text{He}$  is produced with Oxygen in

stars, the primordial value is obtained to regress to the zero metallicity  $O/H \rightarrow 0$  for the observational data. Recently, Fields and Olive [7] reanalyzed the data including the HeI absorption effect and they obtained

$$Y^{obs} = 0.238 \pm (0.002)_{stat} \pm (0.005)_{syst}, \quad (5)$$

where the first error is the statistical uncertainty and the second error is the systematic one. We adopt the above value as the observational  $Y$ .

The primordial  ${}^7\text{Li}/\text{H}$  is observed in the Pop II old halo stars. We adopt the recent measurements by Bonifacio and Molaro [16]

$$\log_{10} \left[ \left( {}^7\text{Li}/\text{H} \right)^{obs} \right] = -9.76 \pm (0.012)_{stat} \pm (0.05)_{syst} \pm (0.3)_{add}. \quad (6)$$

Here we have added the additional uncertainty for fear that  ${}^7\text{Li}$  in halo stars might have been supplemented (by production in cosmic-ray interactions) or depleted (in stars) [17].

It is much more difficult to observe the primordial component of  ${}^6\text{Li}$  because  ${}^6\text{Li}$  is so much rarer than  ${}^7\text{Li}$ . Unfortunately, enough data have not been obtained to find the ‘‘Spite plateau’’ of  ${}^6\text{Li}$ . However, we can set an upper bound on  ${}^6\text{Li}/{}^7\text{Li}$ , since it is generally believed that the evolution of  ${}^6\text{Li}$  is dominated by the production through  $p, \alpha\text{-C, N, O}$  cosmic ray spallation (reactions of cosmic rays with the interstellar medium). Intrinsically the models of the nucleosynthesis through the cosmic ray spallation were motivated to simultaneously agree with whole the observational Li-Be-B abundances [18–20]. On the other hand, recently it was claimed that the observational  ${}^6\text{Li}$  abundance in halo stars is too abundant from the point of view of the cosmic ray energy if  ${}^9\text{Be}$  is fit by the model of the cosmic-ray metal [21]. Therefore, there seems to be some uncertainties in the models of the cosmic ray spallation. In this situation, however, at least it would be safe to assume that  ${}^6\text{Li}$  abundance increases as the metallicity increases. Today we observe only the  ${}^6\text{Li}$  to  ${}^7\text{Li}$  ratio in low-metallicity ( $[\text{Fe}/\text{H}] \leq -2.0$ ) halo stars [22],

$$r_{6,7,halo}^{obs} \equiv ({}^6\text{Li}/{}^7\text{Li})_{halo}^{obs} = 0.05 \pm 0.02. \quad (7)$$

We take this value as an upper bound on the primordial value  $r_{6,7}^{obs}$ ,

$$r_{6,7}^{obs} \leq r_{6,7,halo}^{obs}. \quad (8)$$

### III. PHOTODISSOCIATION AND NON-THERMAL PRODUCTION OF ${}^6\text{Li}$

#### A. Photodissociation

In order to discuss the effect of high-energy photons on BBN, we need the shape of the photon spectrum induced by the primary high-energy photons from the decay of the massive particle  $X$ . In the thermal bath (mixture of photons  $\gamma_{\text{BG}}$ , electrons  $e_{\text{BG}}^-$ , and nucleons  $N_{\text{BG}}$ ), high energy photons lose their energy by the following cascade processes:

- Double-photon pair creation ( $\gamma + \gamma_{\text{BG}} \rightarrow e^+ + e^-$ )

- Photon-photon scattering ( $\gamma + \gamma_{\text{BG}} \rightarrow \gamma + \gamma$ )
- Pair creation in nuclei ( $\gamma + N_{\text{BG}} \rightarrow e^+ + e^- + N$ )
- Compton scattering ( $\gamma + e_{\text{BG}}^- \rightarrow \gamma + e^-$ )
- Inverse Compton scattering ( $e^\pm + \gamma_{\text{BG}} \rightarrow e^\pm + \gamma$ )

In this study we numerically solved the Boltzmann equation including the above processes, and obtained the distribution function of photons,  $f_\gamma(E_\gamma)$ .

The cascade photons induce the photodissociation of the light elements, which modifies the result of standard BBN (SBBN). The evolutions of the light nuclei abundances are governed by the following Boltzmann equation:

$$\begin{aligned} \frac{dn_N}{dt} + 3Hn_N = & \left[ \frac{dn_N}{dt} \right]_{\text{SBBN}} - n_N \sum_{N'} \int dE_\gamma \sigma_{N\gamma \rightarrow N'}(E_\gamma) f_\gamma(E_\gamma) \\ & + \sum_{N''} n_{N''} \int dE_\gamma \sigma_{N''\gamma \rightarrow N}(E_\gamma) f_\gamma(E_\gamma), \end{aligned} \quad (9)$$

where  $n_N$  is the number density of the nuclei  $N$ , and  $[dn_N/dt]_{\text{SBBN}}$  denotes the SBBN contribution to the Boltzmann equation. In Table I, we list the photodissociation processes included in our computation. In this study the model parameters are the baryon to photon ratio ( $\eta$ ), the lifetime of  $X$  ( $\tau_X$ ), the mass of  $X$  ( $m_X$ ), and the yield variable  $Y_X$  of  $X$  after electron-positron annihilation,

$$Y_X = n_X/n_\gamma, \quad (10)$$

where  $n_\gamma$  is the number density of photon.<sup>2</sup> In this paper we assume that  $X$  decays only into photons, i.e.,  $m_X Y_X$  corresponds to  $\Delta\rho_\gamma/n_\gamma$ . Then, the photodissociation rates depend on the combination  $m_X Y_X$  which characterizes the amount of the energy of the injected photons  $\Delta\rho_\gamma$  as far as  $m_X$  is much larger than 20 MeV [31].

## B. Non-thermal ${}^6\text{Li}$ production

As pointed out by Jedamzik [10], both T and  ${}^3\text{He}$  are produced through the photodissociation of  ${}^4\text{He}$ ,

$${}^4\text{He} + \gamma \longrightarrow \begin{cases} n + {}^3\text{He} \\ p + \text{T} \end{cases} \quad (11)$$

They are still energetic and have kinetic energies enough to produce  ${}^6\text{Li}$  through the following processes with the background  ${}^4\text{He}$ :

---

<sup>2</sup>Note that in the reference [3],  $Y_X = n_X/n_\gamma$  is defined before electron-positron annihilation ( $e^+e^-$  ann.). Then they have a relationship  $Y_X|_{\text{after } e^+e^- \text{ ann.}} = \frac{4}{11} Y_X|_{\text{before } e^+e^- \text{ ann.}}$ .

$$T + {}^4\text{He} \longrightarrow {}^6\text{Li} + n, \quad (12)$$

$${}^3\text{He} + {}^4\text{He} \longrightarrow {}^6\text{Li} + p, \quad (13)$$

until they are stopped by the ionization loss through the plasma excitation in the electromagnetic plasma. The threshold energy of the  ${}^6\text{Li}$  production is  $E_{6^3\text{He}}^{th} = 4.03\text{MeV}$  for  ${}^3\text{He}$ , and  $E_{6T}^{th} = 4.80\text{MeV}$  for  $T$ . Then, the abundance of  ${}^6\text{Li}$  produced through the non-thermal (NT) process in Eq. (12) is governed by

$$\left[ \frac{dn_{6\text{Li}}}{dt} \right]_{\text{NT}} = n_{4\text{He}} \int_{E_4^{th} + 4E_6^{th}}^{\infty} dE_{\gamma} \sigma_{4\text{He}(\gamma,p)T}(E_{\gamma}) f_{\gamma}(E_{\gamma}) \int_{E_6^{th}}^{(E_{\gamma} - E_4^{th})/4} n_{4\text{He}} \sigma_{T(\alpha,n)6\text{Li}}(E) \left( \frac{dE}{dx} \right)^{-1} dE, \quad (14)$$

where  $n_{6\text{Li}}(n_{4\text{He}})$  denotes the number density of  ${}^6\text{Li}({}^4\text{He})$ .  $\sigma_{4\text{He}(\gamma,p)T}(E_{\gamma})$  is the cross section of the  ${}^4\text{He}$  photodissociation,  $E_4^{th}$  is the threshold energy of the photodissociation process,  $f_{\gamma}(E_{\gamma})$  is the photon spectrum which are obtained by solving the Boltzmann equation,  $\sigma_{T(\alpha,n)6\text{Li}}(E)$  is the cross section of the process in Eq. (12).  $dE/dx$  denotes the rate of the ionization loss while the charged particle  $T$  is running a distance  $dx$  in the electromagnetic plasma. The rate of the ionization loss is expressed by [32]

$$\frac{dE}{dx} = \frac{Z^2 \alpha}{\beta^2} \omega_p^2 \ln \left( \frac{\Lambda m_e \beta^2}{\omega_p} \right), \quad (15)$$

where  $\omega_p^2$  is plasma frequency ( $= 4\pi n_e \alpha / m_e$ ),  $n_e$  is the electron number density,  $m_e$  is electron mass,  $Z$  is the charge,  $\Lambda \sim \mathcal{O}(1)$  is a constant and  $\beta$  is the velocity. The effect of the process (13) is described by replacing the suffix  $T$  with  ${}^3\text{He}$  in Eq. (14).

We include the above two processes of the non-thermal  ${}^6\text{Li}$  production in BBN code and compute the  ${}^6\text{Li}$  abundance. In the computation we adopt the experimental cross section  $\sigma_{T(\alpha,n)6\text{Li}} = 35 \pm 1.4 \text{ mb}$  [33] commonly for the two processes. Because we have only one data point at the kinetic energy  $E_T = 28 \text{ MeV}$  in the laboratory system, we assume that the cross section is constant for whole the energy region and neglect its energy dependence. Then, we integrate the second factor in Eq. (14) up to a high energy. One can easily find that there exists a serious problem in this procedure if it is compared to the case of the original photodissociation where the photodissociation rates steeply decrease as the energy increases. Because we have the experimental data for the  ${}^4\text{He}$  photodissociation rates only up to about 100 MeV for the photon energy [27–29], we should interpolate the photodissociation rates in a high energy region because of the mild dumping of the integrand. Then, the integration has a large uncertainty ( $\sim 20\%$ ) when we change the upper limit of the integration from 500 MeV to 1 GeV.<sup>3</sup> Therefore, in this situation we adopt 20% errors for the non-thermal  ${}^6\text{Li}$  production rates and perform the Monte Carlo simulation including them.<sup>4</sup>

---

<sup>3</sup>In addition, there may be another larger uncertainty which comes from the differences of the method for the interpolation because we do not know the correct shape of the cross sections. In this case, the obtained constraint would be weaker.

<sup>4</sup>If the cross section  $\sigma_{T(\alpha,n)6\text{Li}}$  decreases at high energy like other nuclear interactions, the  ${}^6\text{Li}$

### C. Constraint from cosmic microwave background

In addition to the photodissociation process, there also exists another constraint. A radiative decay process releases a net photon energy into the electromagnetic plasma. The emitted photons should be thermalized soon, otherwise the photon spectrum deviates from the blackbody, which contradicts the observation of the cosmic microwave background (CMB) [34]. This leads to the following constraints:

$$m_X Y_X \lesssim 2.0 \times 10^{-12} \text{GeV} \left( \frac{\tau_X}{10^{10} \text{sec}} \right)^{\frac{1}{2}}, \quad (16)$$

for  $\mu$ -distortion  $(1.8 \times 10^6 \text{sec} (\Omega_B h^2 / 0.02)^{\frac{2}{3}} \lesssim \tau_X \lesssim 2.3 \times 10^9 \text{sec} (\Omega_B h^2 / 0.02))$ , and

$$m_X Y_X \lesssim 1.9 \times 10^{-12} \text{GeV} \left( \frac{\tau_X}{10^{10} \text{sec}} \right)^{\frac{1}{2}}, \quad (17)$$

for  $y$ -distortion  $(2.3 \times 10^9 \text{sec} (\Omega_B h^2 / 0.02) \lesssim \tau_X \lesssim 10^{12} \text{sec})$ .

### IV. COMPARISON WITH OBSERVATIONAL LIGHT ELEMENT ABUNDANCES

In Fig. 1 we plot the theoretically predicted  ${}^6\text{Li}$  to  ${}^7\text{Li}$  ratio ( $\equiv r_{6,7}^{th}$ ) in  $(\tau_X, m_X Y_X)$  plane. The solid line represents the model parameters which predict the observational mean value of  $r_{6,7}^{th}$  and the dashed line denotes the observational  $2\text{-}\sigma$  upper bound. From the figure, one may think that the mean value of the theoretical prediction constrains  $m_X Y_X$  severely. We should bear in mind, however, that the theoretical prediction has a large uncertainty which comes from the errors of the production rates, and in addition the observational constraint also has a large error. To take account of these uncertainties systematically, we performed the Maximum Likelihood analysis [3] including both the theoretical and the observational errors. Here we assume that the theoretical predictions of  $(\text{D}/\text{H})^{th}$ ,  $Y^{th}$ ,  $\log_{10}[({}^7\text{Li}/\text{H})^{th}]$ ,  $r_{3,2}^{th} = ({}^3\text{He}/\text{D})^{th}$ , and  $r_{6,7}^{th}$  obey the Gaussian probability distribution functions (p.d.f.'s) with the widths given by the  $1\text{-}\sigma$  errors. Concerning the observational values,  $(\text{D}/\text{H})^{obs}$ ,  $Y^{obs}$ , and  $\log_{10}[({}^7\text{Li}/\text{H})^{obs}]$  are assumed to obey the Gaussian p.d.f.'s while we treat  $r_{3,2}^{obs}$  and  $r_{6,7}^{obs}$  as non-Gaussian variables [3].

In Fig. 2 we plot the results of the  $\chi^2$  fitting by using the method of the Maximum Likelihood analysis. The solid (dashed) line denotes the Low D (High D) constraint. The dotted line denotes the upper bound from the CMB constraint. In the figure, the region below the lines are consistent with the observations. The constraint from the CMB is almost always weaker than that from BBN. The main feature of the difference between High D and Low D is that the Low D constraint is severer than High D for a relatively long lifetime case ( $\tau_X \gtrsim 3 \times 10^6 \text{sec}$ ). That is because High D constraint modestly allows the overproduction of  ${}^3\text{He}$  accompanying the  ${}^4\text{He}$  photodissociation. On the other hand, the High D constraint

---

production is less important. As shown later, the resultant constraint is not changed even if we neglect the  ${}^6\text{Li}$  production.

is more stringent for shorter lifetimes since the D dissociation is more important than the  $^4\text{He}$  photodissociation.

The obtained upper bound does not change our earlier results so much [3]. It became slightly weaker because we included the  $\eta$  dependence for the photodissociation rates ( $\Gamma \propto 1/\eta$ ) in this analysis.<sup>5</sup> We find that the non-thermally produced  $^6\text{Li}$  mildly contributes to the bound.<sup>6</sup> The main reason is that both the theoretical computation and observational data have very large uncertainties which amount to about 30 – 40 %.

Assuming that the parent massive particle is the gravitino and that it dominantly decays into a photon and a photino ( $\psi_{3/2} \rightarrow \tilde{\gamma} + \gamma$ ), the lifetime  $\tau_{3/2}$  is related to the gravitino mass  $m_{3/2}$  as

$$\tau_{3/2} \simeq 4 \times 10^5 \text{ sec} \times (m_{3/2}/1 \text{ TeV})^{-3}. \quad (18)$$

Assuming that the gravitino is produced through the thermal scattering in the reheating process after inflation,<sup>7</sup> we relate the abundance  $Y_{3/2} = n_{3/2}/n_\gamma$  of the gravitino with the reheating temperature  $T_R$  [2],

$$Y_{3/2} \simeq 1.1 \times 10^{-11} \times (T_R/10^{10} \text{ GeV}). \quad (19)$$

In Fig. 3 we plot the upper bound on the reheating temperature after inflation at 95% C.L. as a function of the gravitino mass. Here we can read off the constraint by using the relationship of the scaling,  $\Delta\rho_\gamma/n_\gamma = \frac{1}{2}m_{3/2}Y_{3/2}(= m_X Y_X)$  because we assumed X decays into two photons. From the figure we can obtain the upper bound on the reheating temperature:

$$\begin{aligned} m_{3/2} = 100 \text{ GeV} \quad (\tau_{3/2} \simeq 4 \times 10^8 \text{ sec}) : T_R &\lesssim 1 \times 10^7 \text{ GeV}, \\ m_{3/2} = 1 \text{ TeV} \quad (\tau_{3/2} \simeq 4 \times 10^5 \text{ sec}) : T_R &\lesssim 1 \times 10^9 \text{ GeV}, \\ m_{3/2} = 3 \text{ TeV} \quad (\tau_{3/2} \simeq 1 \times 10^4 \text{ sec}) : T_R &\lesssim 9 \times 10^{11} \text{ GeV}, \end{aligned} \quad (20)$$

at 95% C.L.

---

<sup>5</sup>The  $\eta$  dependence is understood as follows. The soft photons produced in the electromagnetic cascade scatter off the background electrons and nucleons and lose their energy. Thus the number density of soft photons with energy larger than the threshold decreases as scattering rate which is proportional to  $\eta$ . Therefore, the photodissociation rates are proportional to  $1/\eta$ .

<sup>6</sup>Tritium is unstable with the lifetime  $\tau_T = 5.614 \times 10^8 \text{ sec}$ , and decays into  $^3\text{He}$  whose charge is two. Thus, because  $^3\text{He}$  subjects to stop easier than T by the ionization loss, we might overestimate the  $^6\text{Li}$  production in parameter regions where the stopping time  $\tau_{stop} = \int_E^0 (dE/dt)^{-1} dE \simeq 2.5 \times 10^9 \text{ sec} (T/\text{eV})^{-3} (E/\text{MeV})^{3/2}$  is longer than the lifetime of Tritium, i.e., for  $T \lesssim 1.7 \text{ eV}$ . Therefore, at a long lifetime  $\tau_X \gtrsim 5 \times 10^{11} \text{ sec}$ , our constraint might become weaker by about factor two. However, it is expected that the effect would not change the result significantly because the  $^3\text{He}$  overproduction gives a severer constraint there.

<sup>7</sup>Although these days it was claimed that gravitinos are also produced in the preheating epoch non-thermally [35–37], we do not consider such processes here because there are some ambiguities on the estimations and they depend on various model parameters. If the non-thermal production is effective, however, the obtained constraint might be severer.



## V. CONCLUSION

In this paper we have studied the effects on primordial nucleosynthesis of the radiative decay of a long-lived massive particle  $X$  using new observational data. We have also considered the non-thermal  ${}^6\text{Li}$  production caused by energetic T and  ${}^3\text{He}$  produced by the  ${}^4\text{He}$  photodissociation. We obtained the photon spectrum through the electromagnetic cascade process by solving a set of Boltzmann equations numerically. In addition, to estimate the theoretical errors we performed Monte Carlo simulation including the theoretical uncertainties which come from those of nuclear reaction rates. To obtain the degree of agreements between theory and observation, we performed the Maximum Likelihood method and the  $\chi^2$  fitting including both the observational and theoretical errors.

As a result we have obtained the upper bound on the abundance  $m_X Y_X$  as a function of its lifetime  $\tau_X$ . The result does not change our previous works significantly. This is because the theoretical and observational errors for  ${}^6\text{Li}$  are significantly large, and it contributes to the constraints more weakly than the  ${}^3\text{He}$  overproduction accompanying the  ${}^4\text{He}$  photodissociation. Therefore, we have concluded that it is premature to emphasize the importance of the non-thermal production of  ${}^6\text{Li}$ .

We have also applied the results obtained by a generic radiatively decaying particle to gravitino  $\psi_{3/2}$ , and we have got the upper bound on the reheating temperature after primordial inflation as a function of the mass,  $T_R \lesssim 10^7 - 10^9$  GeV for  $m_{3/2} = 100$  GeV – 1 TeV (95 % C.L.).

## VI. ACKNOWLEDGMENTS

The work of M.K. is supported by Priority Area 707 “Supersymmetry and Unified Theory of Elementary Particles.” The work of T.M. is supported by the Grant-in-Aid for Scientific Research from the Ministry of Education, Science, Sports and Culture of Japan No. 12047201.

## REFERENCES

- [1] J. Ellis, G.B. Gelmini, J.L. Lopez, D.V. Nanopoulos, and S. Sarkar, Nucl. Phys. **B373**, 399 (1992).
- [2] M. Kawasaki and T. Moroi, Prog. Theor. Phys. **93** 879 (1995).
- [3] E. Holtmann, M. Kawasaki, K. Kohri, and T. Moroi, Phys. Rev. **D60** 023506 (1999).
- [4] B.E.J. Pagel *et al.*, Mon. Not. R. Astron. Soc. **255** (1992) 325.
- [5] K.A. Olive, G. Steigman, and E.D. Skillman, Astrophys. J. **483** (1997) 788.
- [6] Y.I. Izotov, T.X. Thuan, and V.A. Lipovetsky, Astrophys. J. Suppl. Series, **108** (1997) 1; Y.I. Izotov and T.X. Thuan Astrophys. J., **500** (1998) 188.
- [7] B.D. Fields and K.A. Olive, Astrophys. J., **506** 177 (1998).
- [8] S. Burles and D. Tytler, Astrophys. J. **507** 732 (1998).
- [9] D. Tytler, S. Burles, L. Lu, X-M. Fan and A. Wolfe, Astron. J. **117** (1999) 63.
- [10] K. Jedamzik, Phys. Rev. Lett. **84** (2000) 3248.
- [11] S. Dimopoulos, R. Esmailzadeh, L.J. Hall, and G.D. Starkman, Astrophys. J. **330** 545 (1988); Nucl. Phys. **B311** 699 (1989).
- [12] J.M. O'Meara, D. Tytler, D. Kirkman, N. Suzuki, J.X. Prochaska, D. Lubin, and A.M. Wolfe, astro-ph/0011179.
- [13] J. K. Webb *et al.*, Nature **388** (1997) 250.
- [14] J. Geiss, in *Origin and Evolution of the Elements*, edited by N. Prantzos, E. Vangioni-Flam, and M. Cassé (Cambridge University Press, Cambridge, 1993) 89.
- [15] G. Sigl, K. Jedamzik, D.N. Schramm, and V.S. Berezinsky, Phys. Rev. **D52** 6682 (1995), astro-ph/9503094.
- [16] P. Bonifacio and P. Molaro, Mon. Not. R. Astron. Soc. **285** 847 (1997).
- [17] B.D. Fields, K. Kainulainen, K.A. Olive, and D. Thomas, New Astron. **1** (1996) 77, astro-ph/9603009.
- [18] D.K. Duncan, D.L. Lambert, and M. Lemke, Astrophys. J. **401** 584 (1992); M. Cassé, R. Lehoucq, and E. Vangioni-Flam, Nature **373** 318 (1995); R. Ramaty, B. Kozlovsky, and R.E. Lingenfelter, Astrophys. J. Lett. **438** L21 (1995).
- [19] M. Lemoine, D.N. Schramm, J.W. Truran, and C.J. Copi, Astrophys. J. **478** 554 (1997).
- [20] B.D. Fields and K.A. Olive, New Astron. **4** 255 (1999).
- [21] R. Ramaty, S.T. Scully, R.E. Ligenfelter, and B. Kozlovsky, Astrophys. J. **534** 747 (2000).
- [22] V.V. Smith, D.L. Lambert, and P.E. Nissen, Astrophys. J. **408** 262 (1993); L.M. Hobbs and J.A. Thorburn, Astrophys. J. **491** 772 (1997); V.V. Smith, D.L. Lambert, and P.E. Nissen Astrophys. J. **506** 923 (1998); R. Cayrel et al., Astron. Astrophys. **343** 923 (1999).
- [23] R.D. Evans, The Atomic Nucleus (McGraw-Hill, New York, 1955).
- [24] R. Pfeiffer, Z. Phys. **208** (1968) 129.
- [25] D.D. Faul, B.L. Berman, P. Mayer, and D.L. Olson, Phys. Rev. Lett. **44** (1980) 129.
- [26] A.N. Gorbunov and A.T. Varfolomeev, Phys. Lett. **11** (1964) 137.
- [27] J.D. Irish, R.G. Johnson, B.L. Berman, B.J. Thomas, K.G. McNeill, and J.W. Jury, Can. J. Phys. **53** (1975) 802.
- [28] C.K. Malcom, D.V. Webb, Y.M. Shin, and D.M. Skopik, Phys. Lett. **B47** (1973) 433.
- [29] Yu.M. Arkatov, P.I. Vatset, V.I. Voloshchuk, V.A. Zolenko, I.M. Prokhorets, and V.I. Chimil', Sov. J. Nucl. Phys. **19** (1974) 598.

- [30] B.L. Berman, *Atomic Data and Nuclear Data Tables* **15** (1975) 319.
- [31] M. Kawasaki and T. Moroi, *Astrophys. J.* **452**, 506 (1995).
- [32] J.D. Jackson, *Classical Electrodynamics* (Wiley, New York).
- [33] J.A. Koepke and R.E. Brown, *Phys. Rev.* **C16** (1977) 18.
- [34] Fixsen et al., *Astrophys. J.*, **473** 576 (1996).
- [35] R. Kallosh, L Kofman, A Linde, and A.V. Proeyen, *Phys. Rev.* **D61** 103503 (2000).
- [36] G.F. Giudice, A. Riotto, and I. Tkachev, *JHEP* **9908** 009 (1999).
- [37] D.H. Lyth, *Phys. Lett.* **B476** 356 (2000).

# TABLES

	Photodissociation Reactions	1- $\sigma$ Uncertainty	Threshold Energy	Ref.
1.	$D + \gamma \rightarrow p + n$	6%	2.2 MeV	[23]
2.	$T + \gamma \rightarrow n + D$	14%	6.3 MeV	[24,25]
3.	$T + \gamma \rightarrow p + 2n$	7%	8.5 MeV	[25]
4.	${}^3\text{He} + \gamma \rightarrow p + D$	10%	5.5 MeV	[26]
5.	${}^3\text{He} + \gamma \rightarrow n + 2p$	15%	7.7 MeV	[26]
6.	${}^4\text{He} + \gamma \rightarrow p + T$	4%	19.8 MeV	[26]
7.	${}^4\text{He} + \gamma \rightarrow n + {}^3\text{He}$	5%	20.6 MeV	[27,28]
8.	${}^4\text{He} + \gamma \rightarrow p + n + D$	14%	26.1 MeV	[29]
9.	${}^6\text{Li} + \gamma \rightarrow \text{anything}$	4%	5.7 MeV	[30]
10.	${}^7\text{Li} + \gamma \rightarrow 2n + \text{anything}$	9%	10.9 MeV	[30]
11.	${}^7\text{Li} + \gamma \rightarrow n + {}^6\text{Li}$	4%	7.2 MeV	[30]
12.	${}^7\text{Li} + \gamma \rightarrow {}^4\text{He} + \text{anything}$	9%	2.5 MeV	[30]
13.	${}^7\text{Be} + \gamma \rightarrow p + {}^6\text{Li}$	4%		
14.	${}^7\text{Be} + \gamma \rightarrow \text{anything except } {}^6\text{Li}$	9%		

TABLE I. List of photodissociation processes, and the 1- $\sigma$  uncertainty in the cross sections. Since there is no experimental data on photodissociation of  ${}^7\text{Be}$ , we assume that the rate, threshold, and uncertainty for Reaction 13 is the same as for Reaction 11, and the rate for Reaction 14 is the sum of the rates for Reactions 10 and 12.

# FIGURES

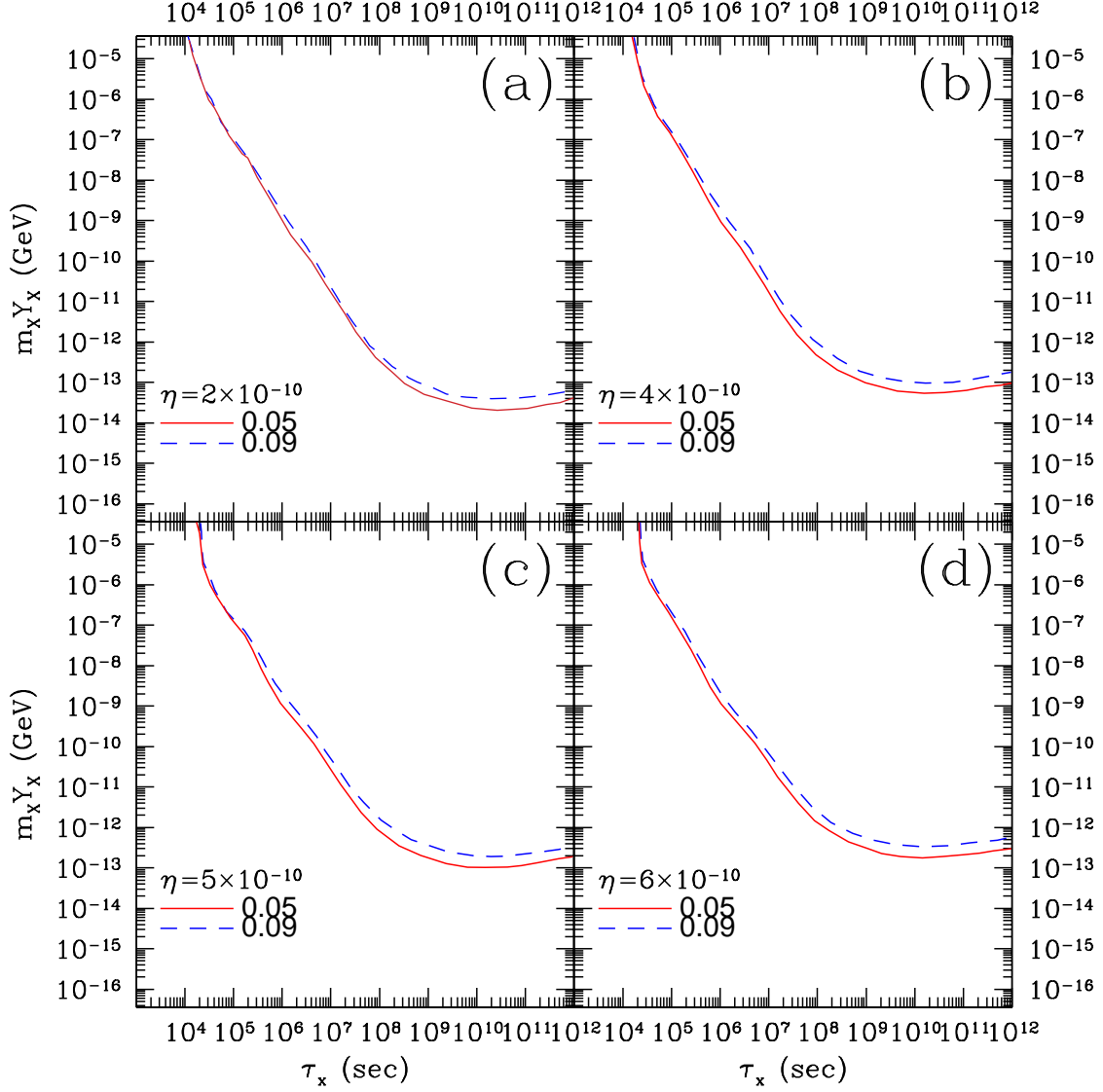


FIG. 1. Plot of  ${}^6\text{Li}$  to  ${}^7\text{Li}$  ratio in  $(\tau_X, m_X Y_X)$  plane for various baryon to photon ratio ( $\eta = n_B/n_\gamma$ ) in (a)  $\eta = 2 \times 10^{-10}$ , (b)  $\eta = 4 \times 10^{-10}$ , (c)  $\eta = 5 \times 10^{-10}$ , and (d)  $\eta = 6 \times 10^{-10}$ . The solid line denotes the observational mean value of  ${}^6\text{Li} / {}^7\text{Li}$  and the dashed line denotes the observational  $2\text{-}\sigma$  upper bound.

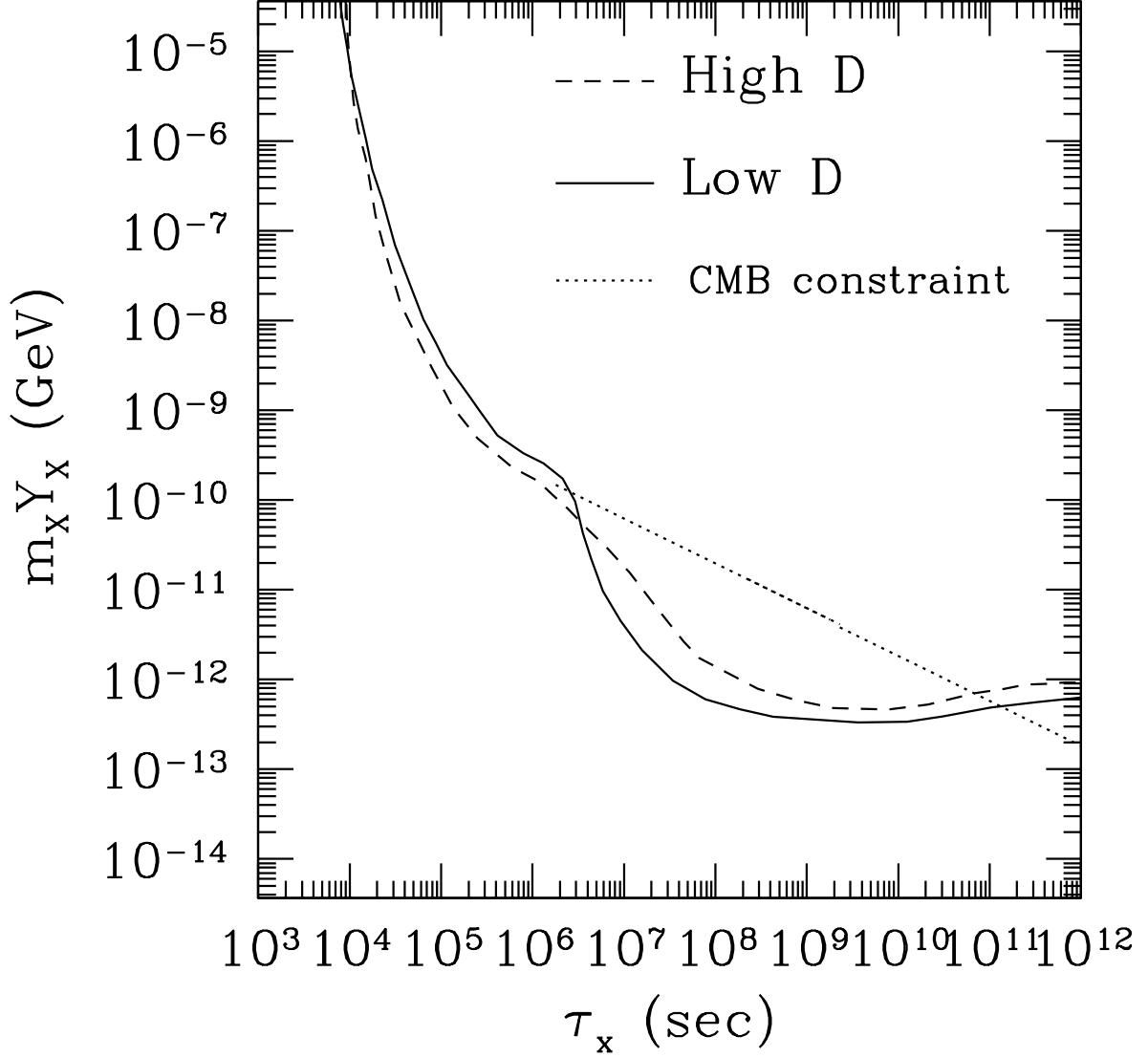


FIG. 2. Plot of the contour of the confidence level in  $(\tau_x, m_X Y_X)$  plane. The solid (dashed) line denotes the 95% C.L. for Low D (High D) projected on  $\eta$  axis. The dotted line denotes the upper bound which comes from CMB constraint.

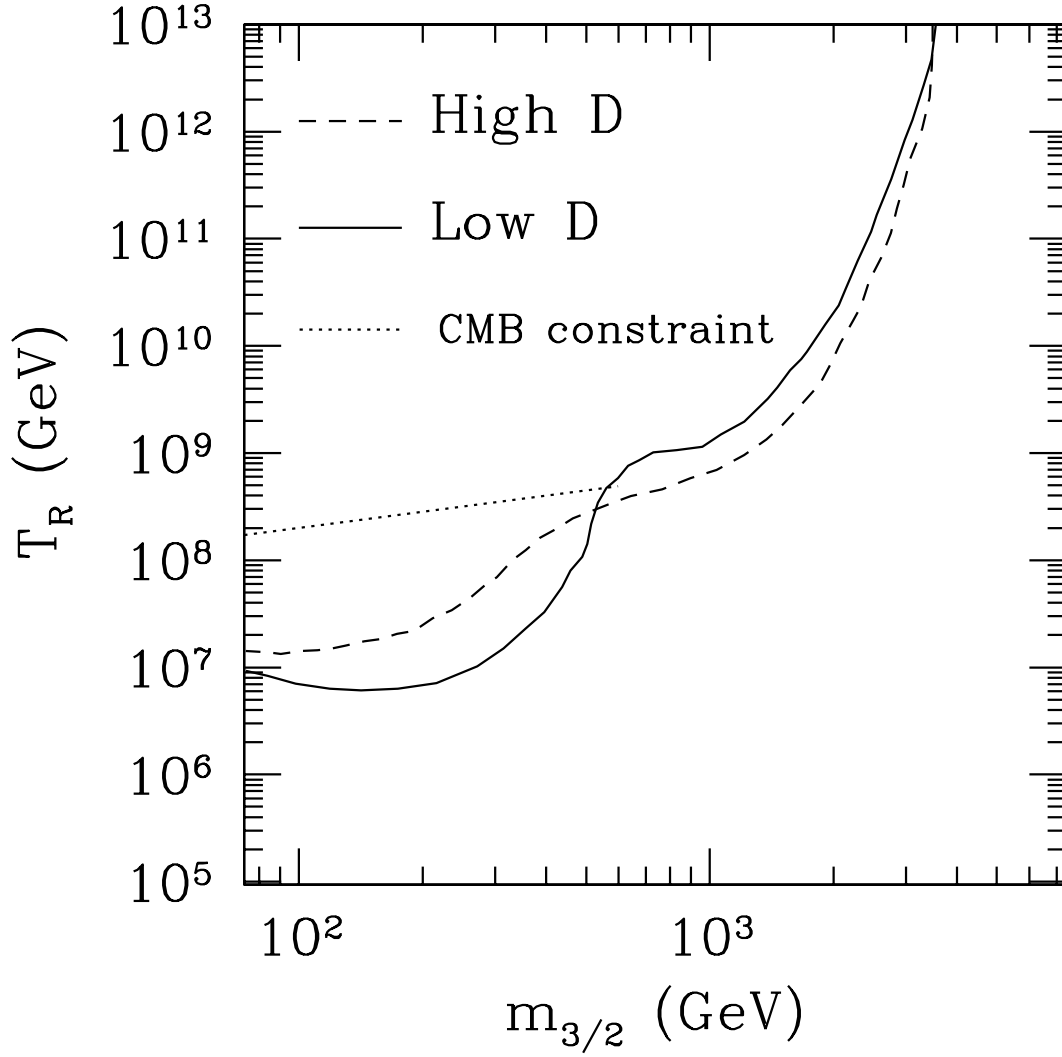


FIG. 3. Plot of the contour of the confidence level in  $(m_{3/2}, T_R)$  plane. The solid (dashed) line denotes the 95% C.L. for Low D (High D). The dotted line denotes the upper bound which comes from CMB constraint.